JOURNAL OF MATERIALS SCIENCE **36** (2001) 4723–4729

Rapid electroplating of photocatalytically highly active TiO_2-Zn nanocomposite films on steel

T. DEGUCHI
Steel R&D Laboratories, Nisshin Steel Co., Ltd., 5, Ishizu-Nishimachi, Sakai, Osaka 592-8332 Japan

K. IMAI
Department of Applied Chemistry, Faculty of Science and Engineering, Kinki University, 3-4-1, Kowakae, Higashi-Osaka, Osaka 577-8502 Japan

H. MATSUI
Molecular Engineering Institute, Kinki University, 3-4-1, Kowakae, Higashi-Osaka, Osaka 577-8502 Japan

M. IWASAKI
Department of Applied Chemistry, Faculty of Science and Engineering, Kinki University, 3-4-1, Kowakae, Higashi-Osaka, Osaka 577-8502 Japan

H. TADA*
Molecular Engineering Institute, Kinki University, 3-4-1, Kowakae, Higashi-Osaka, Osaka 577-8502 Japan
E-mail: h-tada@apch.kindai.ac.jp

S. ITO
Department of Applied Chemistry, Faculty of Science and Engineering, Kinki University, 3-4-1, Kowakae, Higashi-Osaka, Osaka 577-8502 Japan; Molecular Engineering Institute, Kinki University, 3-4-1, Kowakae, Higashi-Osaka, Osaka 577-8502 Japan

Nanocomposite films consisting of TiO_2 and Zn with thickness of 10–15 μm (TiO_2-Zn) have been electrodeposited on steel plates by rapid plating from a $ZnSO_4$-based bath ($I_d > 10$ A dm^{-2}). Upon addition of NH_4NO_3 to the bath (<0.3 g L^{-1}), the uptake of TiO_2 in the film significantly increased. Glow discharge optical emission spectrometry clarified that TiO_2 particles were incorporated throughout the film and the loaded amount increased near the surface. The first-order rate constant (k/h^{-1}) for gas-phase CH_3CHO oxidation was employed as an indicator of the photocatalytic activity. The k value for the TiO_2-Zn film prepared at $I_d = 12$ A dm^{-2} (0.20 h^{-1}) was comparable to that for the sample from a $ZnCl_2$-based bath at $I_d = 4$ A dm^{-2} (0.27 h^{-1}). X-ray diffraction measurements indicated that a TiO_2-ZnO nanocomposite layer was generated on the surface by the heat treatment in air at 673 K for 6 h. Consequently, the photocatalytic activity was further improved ($k = 0.29$ h^{-1}); this effect was explained in terms of the synergy of TiO_2 and ZnO in photocatalysis.

1. Introduction

Nanocomposite films having both the positive attributes of semiconductors in colloidal (large surface area) and thin-film (usability without filtration) forms are expected to be suitable for use as a photocatalyst. The research group of Tacconi and Rajeshwar reported a method of electrodepositing a nanocomposite film consisting of TiO_2 particles and Ni (TiO_2-Ni) on polycrystalline Au electrodes [1, 2]. On the other hand, steel, an essential material in buildings, attracts much interest as a substrate of photocatalytic films competent to purify polluted air and water. Electrodeposition of Zn films on steel is widely practiced for corrosion resistance. We have recently prepared a TiO_2-Zn nanocomposite film on steel from a $ZnCl_2$-based bath at a fairly small current density (I_d) of 4 A dm^{-2} [3]. A high photocatalytic activity was revealed for the sample; however, a more rapid process applicable

*Author to whom all correspondence should be addressed.

to on-line treatment is required from the practical viewpoint.

This paper describes rapid electroplating of TiO_2-Zn nanocomposite films on steel plates from a $ZnSO_4$-based bath ($I_d > 10$ A dm^{-2}). In view of the photocatalytic activity, the optimum conditions for preparing the film are explored.

2. Experimental procedure

2.1. Electroplating of TiO_2-Zn nanocomposite films on steel

Steel with a size of 2.5 cm × 5.0 cm and 0.08 cm in thickness (Nisshin Steel Co. Ltd.) was used as a substrate. Prior to the electrodeposition, steel was washed successively with acetone, a neutral detergent, water and an acidic water (HCl : H_2O = 1 : 1 v/v). The electrodeposition bath contained 350 g L^{-1} $ZnSO_4$, 30 g L^{-1} $(NH_4)_2SO_4$ and TiO_2 particles (average diameter = 6 nm, BET surface area = 260 m^2 g^{-1}, anatase, AMT-100, Tayca Co.); the pH of the bath was adjusted at 4. The concentration of NH_4NO_3 (x/g L^{-1}) and the weight of TiO_2 particles (y/g) were varied at $0 \leq x \leq 0.75$ and $0 \leq y \leq 200$, respectively. Zn (or TiO_2-Zn) films were electrodeposited on steel by flowing a constant current of I_d ($4 \leq I_d \leq 20$ A dm^{-2}) between the steel cathode and a Zn anode at 45°C. The area of the steel electrodeposited and the quantity of electricity were fixed at 25 cm^2 and 720 C, respectively. The nanocomposite film prepared from the bath containing NH_4NO_3 and TiO_2 with respective concentration of x and y was denoted as TiO_2-Zn(x, y)/steel. Post-annealing was carried out in air at 673 K for 2–6 h in order to oxidize the Zn matrix.

2.2. Characterization of the TiO_2-Zn nanocomposite films

The Zn in the TiO_2-Zn film (12.5 cm^2) was firstly dissolved into a HCl aq. solution (20 mL, conc. HCI: H_2O = 1:1 v/v), and then 10 mL of a H_2SO_4 aq. solution (conc. H_2SO_4 : H_2O = 1 : 1 v/v) was added and heated to dissolve the TiO_2 particles completely. After the homogeneous solution had been further diluted to 50 mL with H_2O, it was analyzed by induced coupled plasma spectroscopy (ICPS-1000, Shimadzu) to determine the amount of the TiO_2 uptake.

X-ray diffraction (XRD) patterns of TiO_2-Zn/steel samples were obtained on a Rigaku RINT 2500. The measurements were performed in the range of 5°–105° at 8° min^{-1} using Cu-K_α as a x-ray source (40 kV-80 mA).

Diffuse reflectance spectra of the samples were measured using a Hitachi U-400 spectrophotometer in the wavelength range between 300 and 500 nm. The reflectance was recorded with respect to a reference of Al_2O_3.

Depth profiles of the TiO_2-Zn film compositions were determined using a glow discharge optical emission spectrometer (GDOES, Rigaku GDS-3860). The measurements were carried out at a power of 30 W under an Ar flow (180 mL min^{-1}). The inner diameter of the anode was 4 mm.

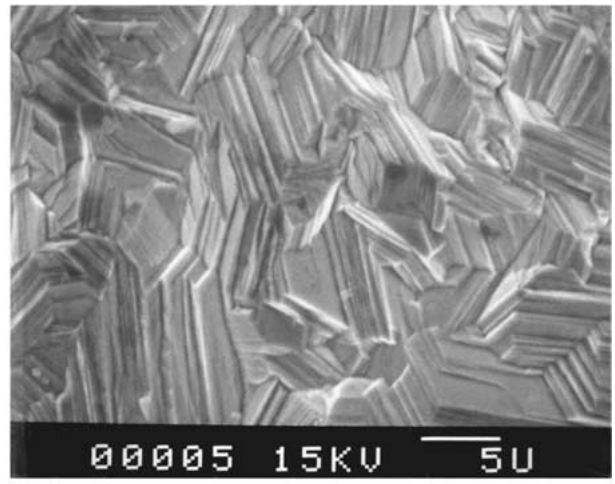

(A)

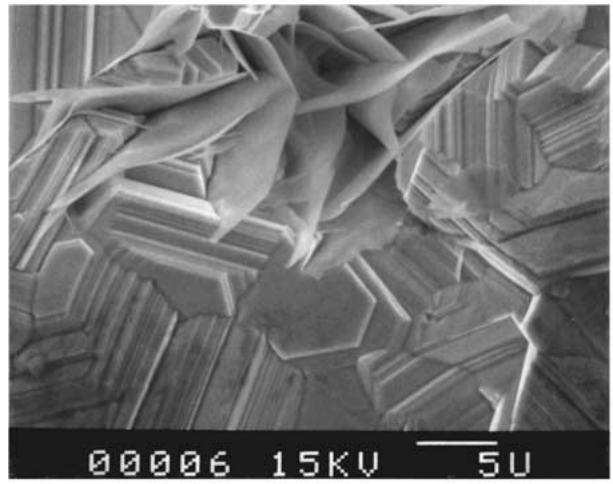

(B)

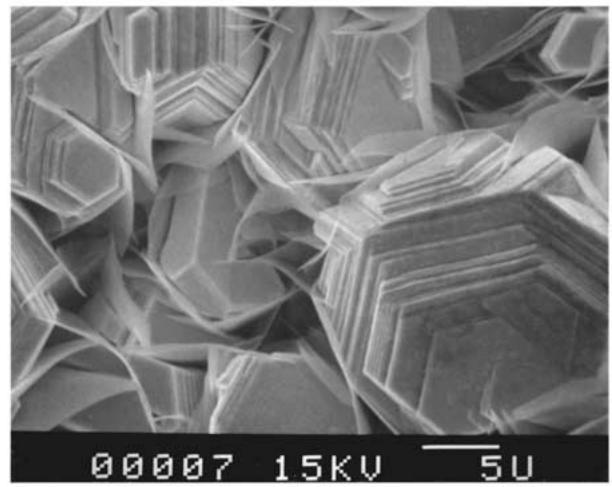

(C)

Figure 1 SEMs of Zn/steel samples prepared at I_d = 20 A dm^{-2}: A, x = 0; B, x = 0.2; C, x = 0.3.

2.3. Evaluation of photocatalytic activity

The photocatalytic activities of TiO_2-Zn/steel samples in the oxidation of CH_3CHO were measured [4, 5].

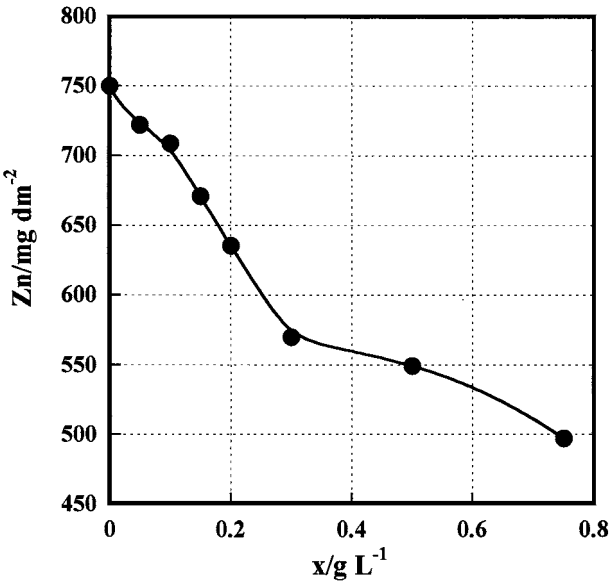

Figure 2 Plots of the weight of Zn vs. x: electricity = 720 C.

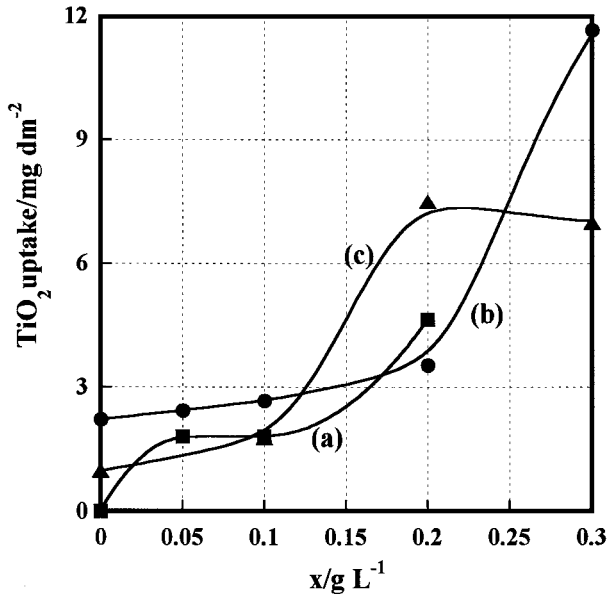

Figure 4 Dependence of the loaded amounts of TiO_2 on x: a, I_d = 8 A dm^{-2}; b, I_d = 12 A dm^{-2}; c, I_d = 20 A dm^{-2}. y was fixed at 100.

A 500-ppm standard CH_3CHO gas (CH_3CHO/N_2) was introduced into a reaction chamber (0.64 L), and diluted with air so that its initial concentration was controlled within the 200 ± 50 ppm range. After the adsorption equilibrium of CH_3CHO had been achieved in the dark, front-face irradiation ($\lambda > 300$ nm, $I_{320-400} = 2.9$ mW cm^{-2}) of the sample (apparent surface area = 19.6 cm^2) was carried out using a 300 W Xe lamp (Wacom, model XDS-301S) at room temperature. The concentration of CH_3CHO was determined by gas chromatography (Shimadzu GC-14B).

3. Results and discussion

3.1. NH_4NO_3 additive effect on the Zn electroplating

The effect of NH_4NO_3 addition to the bath on the Zn electroplating was examined with its amount varied. Fig. 1 shows the scanning electron micrographs (SEMs) of Zn/steel samples prepared at I_d = 20 A dm^{-2}: A, $x = 0$; B, $x = 0.2$; C, $x = 0.3$. Sample A is a dense polycrystalline film consisting of many hexagonal platelets. Sample B has holes surrounded by thin leaves, and the number of the holes increases

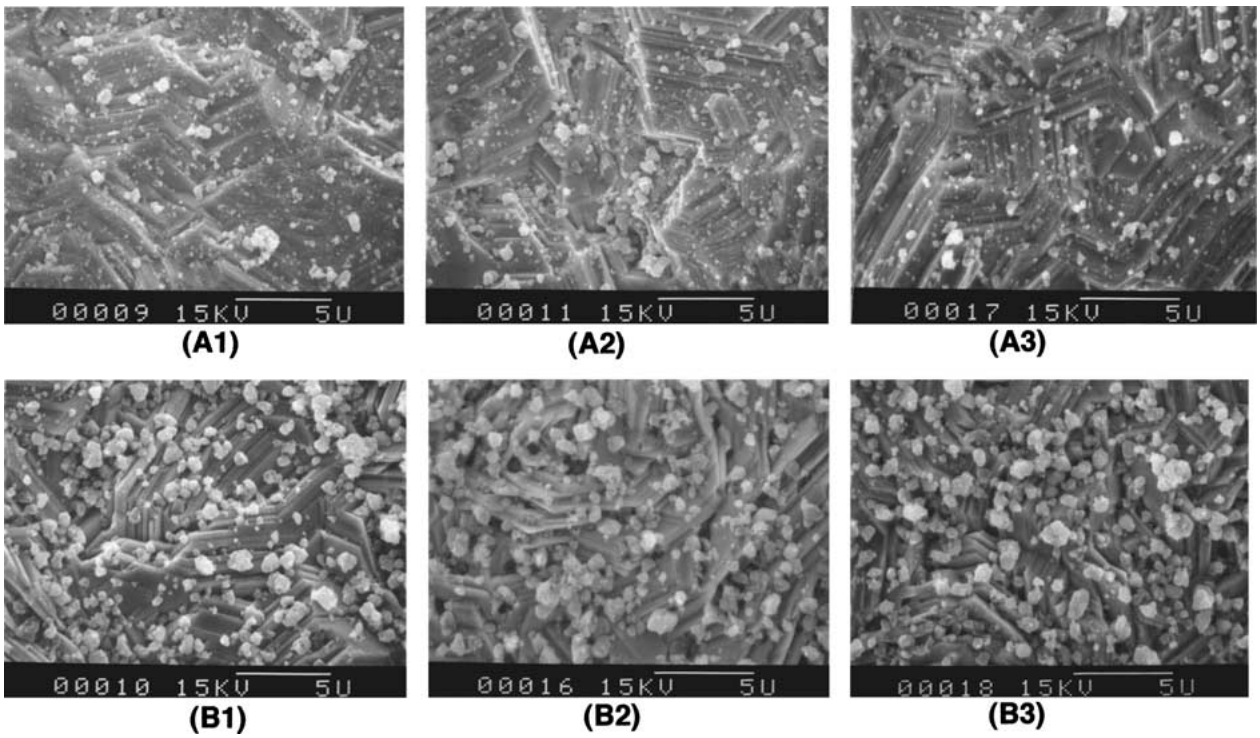

Figure 3 A, SEMs of TiO_2-Zn(0,100)/steel samples: A1, I_d = 8 A dm^{-2}; A2, I_d = 12 A dm^{-2}; A3, I_d = 20 A dm^{-2}. B, SEMs of TiO_2-Zn(0.3,100)/steel samples: B1, I_d = 8 A dm^{-2}; B2, I_d = 12 A dm^{-2}; B3, I_d = 20 A dm^{-2}.

(A)

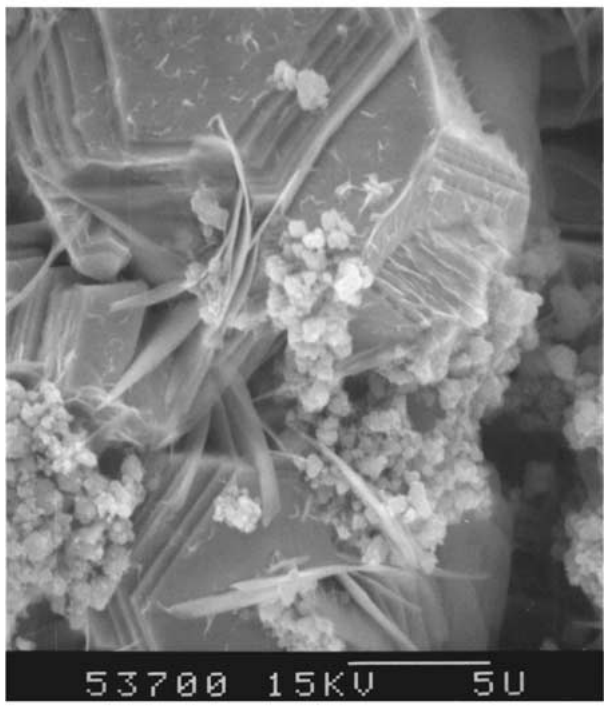

(B)

Figure 5 Surface SEM images for the TiO_2-Zn nanocomposite films prepared at $I_d = 8$ A dm^{-2}: A, TiO_2-Zn(0.1,10)/steel; B, TiO_2/Zn(0.5,10)/steel.

in sample C. A similar trend was observed for samples formed at $I_d = 8$ and 12 A dm^{-2}. Fig. 2 shows the weight of Zn electrodeposited at constant electricity of 720 C as a function of x ($0 \leq x \leq 0.75$). The amount of Zn decreases monotonically with an increase in x. The electroplating efficiencies (η) for $x = 0$ and $x = 0.3$ were calculated to be 77% and 58%, respectively, by using these data. Since some redox reactions of NO_3^- ions have more positive standard electrode potentials (E^0) than that for the redox couple of Zn^{2+}/Zn (Equation 1) [6], the decrease in η may result from the side reactions involving one expressed by Equation 2.

$$Zn^{2+} + 2e^- \leftrightarrow Zn \qquad E^0 = -0.763 \text{ V vs SHE} \tag{1}$$

$$NO_3^- + 4H^+ + 3e^- \leftrightarrow NO + 2H_2O \qquad E^0 = +0.96 \text{ V vs SHE} \quad \text{at pH} = 4.5 \tag{2}$$

3.2. Additive effect of NH_4NO_3 on the TiO_2-Zn nanocomposite electroplating

Fig. 3A shows the SEMs of TiO_2-Zn(0,100)/steel samples: A1, $I_d = 8$ A dm^{-2}; A2, $I_d = 12$ A dm^{-2}; A3, $I_d = 20$ A dm^{-2}. In every sample, a number of TiO_2 particles smaller than ca. 1 μm are dispersed on the surface of the Zn film. Fig. 3B are the SEMs of TiO_2-Zn(0.3,100)/steel samples: B1, $I_d = 8$ A dm^{-2}; B2, $I_d = 12$ A dm^{-2}; B3, $I_d = 20$ A dm^{-2}. The addition of NH_4NO_3 significantly increases both the average size and the uptake of TiO_2 aggregates. Further, the amount of TiO_2 incorporated into the film was determined by ICPS. Fig. 4 shows the variation of the TiO_2 amount as a function of x ($y = 100$): a, $I_d = 8$ A dm^{-2}; b, $I_d = 12$ A dm^{-2}; c, $I_d = 20$ A dm^{-2}. Irrespective of current density, the amount of TiO_2 increases with increasing x at $0 \leq x \leq 0.3$. A maximum amount of TiO_2 incorporated from the $ZnSO_4$-based bath is obtained under conditions of $I_d = 12$ A dm^{-2}, $x = 0.3$ and $y = 100$ (11.8 mg dm^{-2}), which is smaller than that from the $ZnCl_2$-based bath by a factor of ca. 3 [7]. Fig. 5 shows the surface SEM images for the TiO_2-Zn nanocomposite films prepared at $I_d = 8$ A dm^{-2}: A, TiO_2-Zn(0.1,10)/steel; B, TiO_2/Zn(0.5,10)/steel. Apparently, TiO_2 particles are preferentially incorporated into the holes generated by the NH_4NO_3 addition. This seems to be the main reason for the increase in the loaded amount of TiO_2 with the addition of NH_4NO_3. Fig. 6 shows the GDOES depth profiles for the TiO_2-Zn nanocomposite films prepared at $I_d = 12$ A dm^{-2}: A, TiO_2-Zn(0.3,100)/steel; B, TiO_2-Zn(0,100)/steel. Depth profile B demonstrates that a small amount of TiO_2 particles is present only near the surface of the film. In sample A, Ti is distributed throughout the film, and its signal intensity remarkably increases as it approaches the surface.

3.3. Heat treatment of TiO_2-Zn nanocomposite films

The crystallinity change of the TiO_2-Zn nanocomposite film with heat treatment was examined. Fig. 7 shows the XRD patterns for the films: a, TiO_2-Zn(0.3,100)/steel; b, TiO_2-Zn(0.3,100)/steel heated at 673 K for 6 h; c, Zn(0.3,0)/steel heated at 673 K for 6 h. In sample (a), a diffraction peak from the (101) plane of anatase is observed at $2\theta = 25.3^\circ$ together with several peaks due to Zn crystals. In pattern (b), all the peaks of Zn

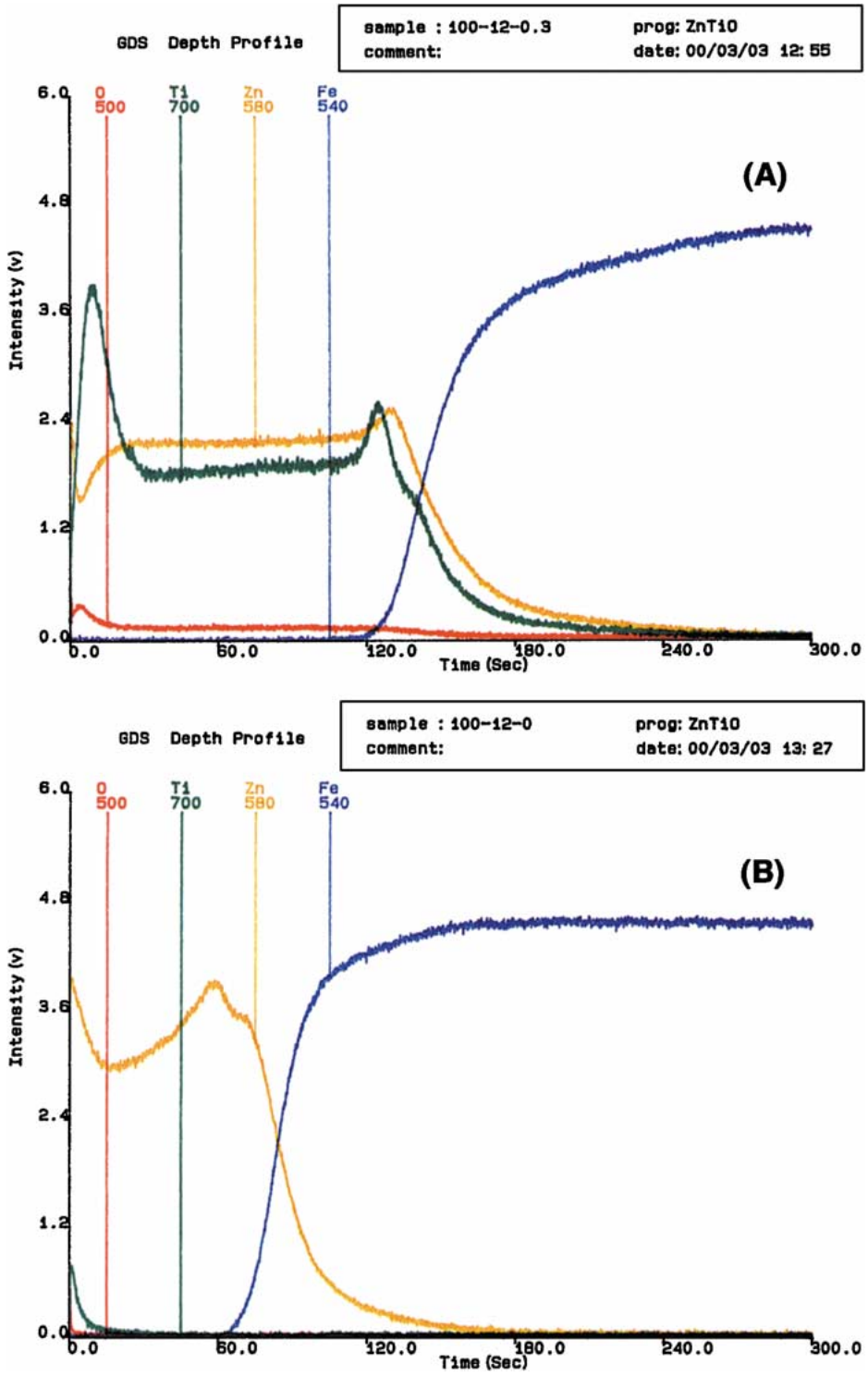

Figure 6 GDOES depth profiles for the TiO_2-Zn nanocomposite films prepared at $I_d = 12$ A dm^{-2}: A, TiO_2-Zn(0.3,100)/steel; B, TiO_2-Zn(0,100)/steel.

disappear, and new peaks assignable to those of hexagonal ZnO crystals appear [8]. The latter peak positions are in complete agreement with those in pattern (c). These findings indicate that the surface of sample (b) consists of a nanocomposite of TiO_2 and ZnO (TiO_2-ZnO(x, y)/steel). Fig. 8 shows diffuse reflectance spectra of the following samples: a, Zn(0.3.0)/steel; b, TiO_2-Zn(0.3,100)/steel; c, ZnO(0.3,0)/steel; d, TiO_2-ZnO(0.3100)/steel. Spectrum (a) indicates high reflectivity (>60%) characteristic of metals in the 300–500 nm range. In spectrum (b), the band gap transition of anatase TiO_2 (band gap, $E_g \cong 3.2$ eV) is responsible for the decrease in reflectivity at $\lambda < 385$ nm [9]. Also, the decrease of reflectivity at $\lambda < 400$ nm in spectrum (c) results from the band gap absorption of ZnO crystals (Fig. 7c). Since the E_g of ZnO is equal to that of TiO_2 [9] , the redshift of the absorption edge by 15 nm (400 nm–385 nm) may be induced by oxygen vacancy of ZnO [10]. The significant decrease in reflectivity at $\lambda < 420$ nm in spectrum (d) is ascribable

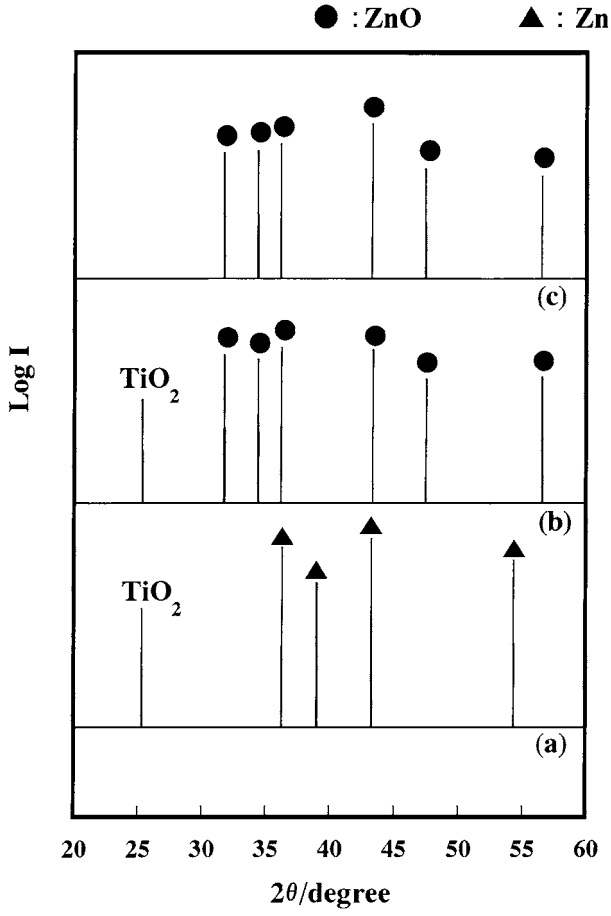

Figure 7 XRD patterns for the films: a, TiO_2-Zn(0.3,100)/steel; b, TiO_2-Zn(0.3,100)/steel heated at 673 K for 6 h; c, Zn(0.3,0)/steel heated at 673 K for 6 h.

to the overlap of the absorption of TiO_2 and ZnO. The further redshift of the absorption edge by 20 nm (420 nm–400 nm) suggests that the high population of the TiO_2 particles on the surface (Fig. 6A) suppresses the oxidation of Zn surfaces. This in turn explains the high reflectivity at $\lambda > 420$ nm.

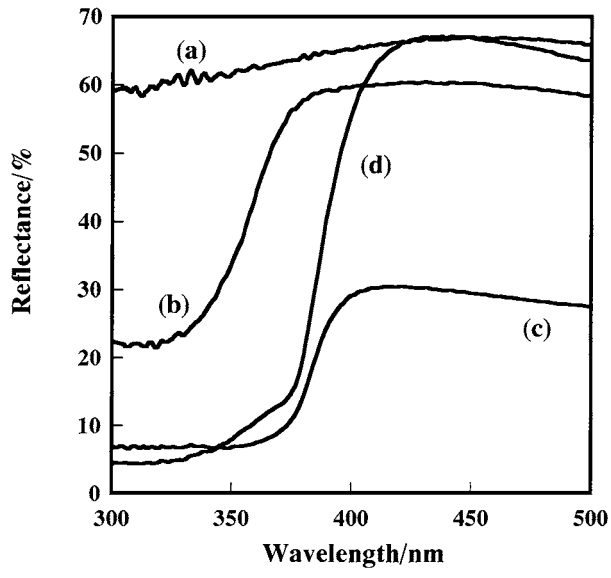

Figure 8 Diffuse reflectance spectra of the following samples: a, Zn(0.3.0)/steel; b, TiO_2-Zn(0.3,100)/steel; c, ZnO(0.3,0)/steel; d, TiO_2-ZnO(0.3100)/steel.

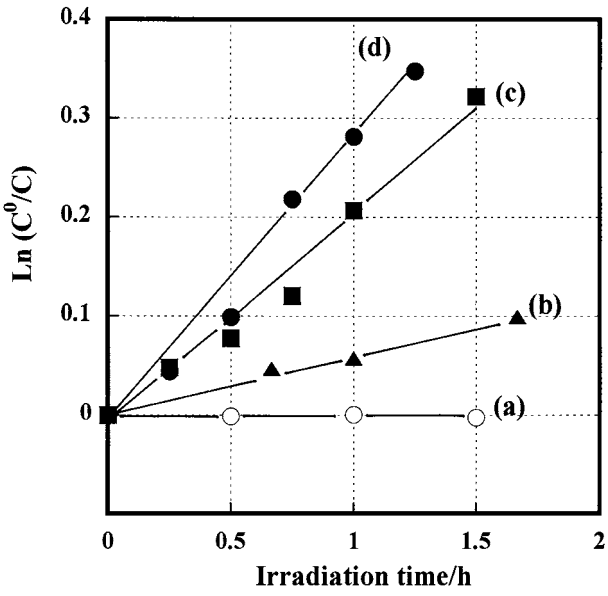

Figure 9 Photocatalytic activities of several samples produced at $I_d = 12$ A dm^{-2} for CH_3CHO decomposition: (a), Zn(0.3,0)/steel; (b), ZnO(0.3,0)/steel; (c), TiO_2-Zn(0.3,100)/steel; (d), TiO_2-ZnO(0.3, 100)/steel. C° and C denote the concentrations of CH_3CHO at $t = 0$ and $t = t$, respectively.

3.4. Photocatalytic activity of TiO_2-Zn nanocomposite films

Fig. 9 shows the photocatalytic activities of several samples produced at $I_d = 12$ A dm^{-2} for CH_3CHO decomposition: (a), Zn(0.3,0)/steel; (b), ZnO(0.3,0)/steel; (c), TiO_2-Zn(0.3,100)/steel; (d), TiO_2-ZnO(0.3,100)/steel. C° and C denote the concentrations of CH_3CHO at $t = 0$ and $t = t$, respectively. In every system, the plots yields a straight line with a slope giving an apparent rate constant (k). No decomposition of CH_3CHO occurs in system (a). The fact that both TiO_2 (and/or ZnO) and illumination ($\lambda > 300$ nm) are required for the CH_3CHO decomposition suggests that this reaction is induced by the band gap excitation of TiO_2 (and/or ZnO). In system (b), the concentration of CH_3CHO decreases with illumination ($k = 0.06$ h^{-1}); this can be attributed to the photocatalytic activity of ZnO generated as the result of surface oxidation. It is known that ZnO has a photocatalytic activity for the oxidation of CH_3CHO [11]. Sample (c) has a considerably higher activity due to TiO_2 particles incorporated into the film ($k = 0.20$ h^{-1}). Noticeably, the activity of sample (d) ($k = 0.29$ h^{-1}) is further greater than that of sample (c). The sum of the k values of samples (b) and (c) is almost equal to the k value of sample (d). This finding suggests that ZnO as well as TiO_2 acts as a photocatalyst in sample (d), whereas Zn is only a matrix for fixing TiO_2 particles in sample (c).

4. Conclusions

TiO_2-Zn nanocomposite films were successfully formed on steel plates by rapid plating from a $ZnSO_4$-based bath ($I_d > 10$ A dm^{-2}). The addition of NH_4NO_3 to the bath significantly increased the uptake of TiO_2 in the film. The GDOES analyses clarified that TiO_2 particles are incorporated throughout the film and its

amount increases near the surface. The resultant film exhibited a photocatalytic activity for CH_3CHO oxidation comparable to that of the sample prepared from a $ZnCl_2$-based bath at $I_d = 4$ A dm^{-2}. Heat treatment at 673 K for 6 h generated a TiO_2-ZnO nanocomposite layer on the surface, improving the photocatalytic activity further. This effect was explained in terms of the synergy of TiO_2 and ZnO in photocatalysis. This research has presented a feasible method for endowing a high photocatalytic activity with steel plates.

References

1. M. ZHNOU, W.-Y. LIN, N. R. DE TACCONI and K. RAJESHWAR, *J. Electroanal. Chem.* **402** (1996) 221.
2. M. ZHOU, N. R. DE TACCONI and K. RAJESHWAR, *ibid.* **421** (1997) 111.
3. S. ITO, T. DEGUCHI, K. IMAI, M. IWASAKI and H. TADA, *Electrochem. Solid-State Lett.* **2** (1999) 440.
4. M. L. SAUER and D. F. OLLIS, *J. Catal.* **158** (1996) 570.
5. D. S. MUGGLI, J. T. McCUE and J. L. FALCONER, *J. Catal.* **173** (1998) 470.
6. A. FUJISHIMA, M. AIZAWA and T. INOUE, "Denkikagaku Sokuteiho" (Gihodo Pub., Tokyo, 1984).
7. T. DEGUCHI, K. IMAI, M. IWASAKI, H. TADA and S. ITO, *J. Electrochem. Soc.* **147** (2000) 2263.
8. JCPDS card No. 36-1451.
9. E. PELIZZETTI and M. VISCA, in "Energy Resources through Photochemistry and Catalysis," edited by M. GRAETZEL (Academic Press, New York, 1983).
10. Y. KUBOKAWA, M. ANPO, K. HONDA and K. ITO, in "Hikarishokubai (Photocatalysts)", edited by Y. KUBOKAWA, K. HONDA and Y. SAITO (Asakurashoten, Tokyo, 1988).
11. Y. YAMAGUCHI, M. YAMAZAKI, S. YOSHIHARA and T. SHIRAKASHI, *J. Electroanal. Chem.* **442** (1998) 1.

Received 10 July 2000
and accepted 4 May 2001